RAY-BORN SYNTHETIC SEISMOGRAMS FOR COMPLEX STRUCTURES CONTAINING SCATTERERS

VLASTISLAV ČERVENÝ [1,2] and ANASTASIA COPPOLI D.M. [2]

[1] *Institute of Geophysics, Charles University, Ke Karlovu 3, 121 16 Praha 2, Czechoslovakia.*
[2] *Instituto de Geociências, Universidade Federal da Bahia, Rua Caetano Moura 123, Federação, 40.210 Salvador, Bahia, Brasil.*

(Received November 29, 1991; revised version accepted January 3, 1992)

ABSTRACT

Červený, V. and Coppoli D.M., A., 1992. Ray-Born synthetic seismograms for complex structures containing scatterers. *Journal of Seismic Exploration*, 1: 191-206.

The hybrid method based on a combination of the ray theory with the Born approximation can be used to compute synthetic seismograms in complex, laterally varying layered structures containing small scatterers. The scatterers can be combined to form objects of a complex shape. The wave field in the background, laterally varying layered structure is computed by the ray method and the single scattered wave field by the Born approximation. A computer program package designed for such hybrid ray-Born computations in 2-D models is briefly described and numerical applications are presented. The ray-Born numerical modelling of seismic wave fields extends the possibilities of ray modelling considerably.

KEY WORDS: ray method, Born approximation, hybrid ray-Born method, scattering of seismic waves.

INTRODUCTION

The ray method has found many successful applications in seismic prospecting for oil and in seismology. It is very general and can be used to study the propagation of high-frequency seismic (or acoustic) waves in complex, laterally varying layered structures. Even though the accuracy of the ray method is only limited, it is the only method that is able to give an approximate answer to many wave propagation problems in 2-D and 3-D complex structures of a great practical importance.

0963-0651/92/$5.00

The ray method, however, can be applied only to wave fields in media with smooth variations of elastic parameters and density. The model may contain interfaces, but these interfaces must be also smooth. In regions of high velocity gradient, the ray method is not applicable. Similarly,the ray method is not directly applicable to study the interaction of the wave field with scatterers, the size of which is less than or comparable with the wavelength.

The scattered wave field generated by such scatterers can, however, be studied by other methods. If the velocities and the density within the scatterers do not differ considerably from the velocities and the densities in the surrounding media, the perturbation methods can be used, for example the Born or the Rytov appoximation.

Here we discuss the hybrid method based on a combination of the ray method and the Born approximation. We consider a general smooth, laterally varying layered structure, in which the ray method can be used. This structure is considered as a background medium. In addition, the structure contains a limited number of scatterers. The single scattered wavefield is then evaluated by the Born integrals.

In this contribution, we briefly describe both the ray and the Born computations for a general 3-D background model containing scatterers. For simplicity, we consider here only acoustic media; the generalization for elastic media is straightforward. We also briefly describe the computer program package used for the ray-Born numerical modelling of acoustic wavefields in complex 2-D stuctures, and present examples of computations.

ACOUSTIC RAY THEORY GREEN FUNCTION

The pressure wave field $p(\mathbf{x},t)$ satisfies in inhomogeneous medium the acoustic wave equation

$$\nabla\cdot(\sigma\nabla p) - \varkappa\ddot{p} = -\dot{q}(\mathbf{x},t), \tag{1}$$

where t is time, $\mathbf{x} \equiv (x_1, x_2, x_3)$ are Cartesian coordinates, $\varkappa(\mathbf{x})$ the compressibility, $\sigma(\mathbf{x})$ the specific volume and $q(\mathbf{x},t)$ the volume injection rate density. The dots above the letters denote partial derivatives with respect to time. Instead of σ and $\varkappa$, we can also use the density $\varrho(\mathbf{x})$ and the propagation velocity $c(\mathbf{x})$ using the following relations: $\sigma = 1/\varrho$, $\varkappa = 1/\varrho c^2$. We define the acoustic Green function $G(\mathbf{x},t\,;\mathbf{x}_0,t_0)$ as a solution of (1) at a point $\mathbf{x}$ and time t corresponding to the source function $\dot{q}(\mathbf{x},t)$ given by the relation

$$\dot{q}(\mathbf{x},t) = \delta(t - t_0)\,\delta(\mathbf{x} - \mathbf{x}_0). \tag{2}$$

Thus, the acoustic Green function satisfies the equation

$$\nabla\cdot(\sigma\nabla G) - \varkappa\ddot{G} = -\delta(t - t_0)\,\delta(\mathbf{x} - \mathbf{x}_0). \tag{3}$$

The Green function can be calculated by ray methods for very general 3-D laterally varying layered structures. At interfaces, proper interface conditions must be taken into account (continuity of the pressure and of the normal component of the particle velocity). Then the ray theory acoustic Green function is described by the following equation

$$G(\mathbf{x},t\,;\,\mathbf{x}_0,t_0) = \sum_{(\Omega)} G^{\Omega}(\mathbf{x},t\,;\,\mathbf{x}_0,t_0)\,, \tag{4}$$

where the summation runs over all rays Ω connecting $\mathbf{x}$ and $\mathbf{x}_0$, corresponding to direct, reflected, multiply reflected, and other types of waves. The number of rays connecting $\mathbf{x}$ and $\mathbf{x}_0$ may be finite or infinite. If the number is infinite, the series (4) must be truncated. The Green function $G^{\Omega}(\mathbf{x},t\,;\,\mathbf{x}_0,t_0)$, corresponding to a selected ray Ω, will be called here the elementary Green function. It is given by the following equation

$$G^{\Omega}(\mathbf{x},t\,;\,\mathbf{x}_0,t_0) = \mathrm{Re}[\,A^{\Omega}(\mathbf{x},\mathbf{x}_0)\delta^{(A)}\{t - t_0 - T^{\Omega}(\mathbf{x},\mathbf{x}_0)\}]. \tag{5}$$

Here $\delta^{(A)}(\xi)$ is an analytic delta function and $T^{\Omega}(\mathbf{x},\mathbf{x}_0)$ is the travel time from $\mathbf{x}_0$ to $\mathbf{x}$ along the ray Ω. The analytic delta function is given by the well-known relation $\delta^{(A)}(\xi) = \delta(\xi) - i/(\pi\xi)$, where $\delta(\xi)$ is a standard real-valued delta function. The travel time $T^{\Omega}(\mathbf{x},\mathbf{x}_0)$ can be calculated by ray tracing. The complex-valued amplitude factor $A^{\Omega}(\mathbf{x},\mathbf{x}_0)$ is given by the relation

$$A^{\Omega}(\mathbf{x},\mathbf{x}_0) = [\rho(\mathbf{x})\rho(\mathbf{x}_0)c(\mathbf{x})c(\mathbf{x}_0)]^{1/2}\,\mathrm{Re}^{\,i\,\delta T(\mathbf{x},\mathbf{x}_0)} \,/\, 4\pi J(\mathbf{x},\mathbf{x}_0)\,. \tag{6}$$

Here the function $J(\mathbf{x},\mathbf{x}_0)$ is the relative geometrical spreading. It can be calculated by dynamic ray tracing along the ray Ω, performed in the ray-centred coordinates. By the solution of the dynamic ray-tracing system along Ω from

$\mathbf{x}_0$ to $\mathbf{x}$, we can determine the 4×4 ray propagator matrix $\mathbf{\Pi}(\mathbf{x}, \mathbf{x}_0)$ which satisfies at $\mathbf{x} = \mathbf{x}_0$ the initial conditions $\mathbf{\Pi}(\mathbf{x}_0, \mathbf{x}_0) = \mathbf{I}$, where $\mathbf{I}$ is a 4×4 identity matrix. We introduce four 2×2 matrices $\mathbf{P}_1(\mathbf{x}, \mathbf{x}_0)$, $\mathbf{Q}_1(\mathbf{x}, \mathbf{x}_0)$, $\mathbf{P}_2(\mathbf{x}, \mathbf{x}_0)$ and $\mathbf{Q}_2(\mathbf{x}, \mathbf{x}_0)$ by the following equation

$$\mathbf{\Pi}(\mathbf{x}, \mathbf{x}_0) = \begin{bmatrix} \mathbf{Q}_1(\mathbf{x}, \mathbf{x}_0) & \mathbf{Q}_2(\mathbf{x}, \mathbf{x}_0) \\ \mathbf{P}_1(\mathbf{x}, \mathbf{x}_0) & \mathbf{P}_2(\mathbf{x}, \mathbf{x}_0) \end{bmatrix}. \tag{7}$$

Then the relative geometrical spreading $J(\mathbf{x}, \mathbf{x}_0)$ is given by the relation

$$J(\mathbf{x}, \mathbf{x}_0) = |\det \mathbf{Q}_2(\mathbf{x}, \mathbf{x}_0)|. \tag{8}$$

It is possible to show that the relative geometrical spreading $J(\mathbf{x}, \mathbf{x}_0)$ is reciprocal,

$$J(\mathbf{x}, \mathbf{x}_0) = J(\mathbf{x}_0, \mathbf{x}), \tag{9}$$

and that it does not depend on the parametrisation of the ray field. The function $\delta T(\mathbf{x}, \mathbf{x}_0)$ in (6) is the phase shift due to caustics and can be also calculated by dynamic ray tracing. In a homogeneous medium, $J(\mathbf{x}, \mathbf{x}_0)$ and $\delta T(\mathbf{x}, \mathbf{x}_0)$ can be determined analytically, $J(\mathbf{x}, \mathbf{x}_0) = c^2 |\mathbf{x} - \mathbf{x}_0|^2$ and $\delta T(\mathbf{x}, \mathbf{x}_0) = 0$. For a 2-D case, the matrix $\mathbf{Q}_2(\mathbf{x}, \mathbf{x}_0)$ has a diagonal form and the relative geometrical spreading can be expressed as follows:

$$J(\mathbf{x}, \mathbf{x}_0) = |Q_2''(\mathbf{x}, \mathbf{x}_0)|\, \sigma(\mathbf{x}, \mathbf{x}_0), \tag{10}$$

where $\sigma(\mathbf{x}, \mathbf{x}_0)$ is given by the relation,

$$\sigma(\mathbf{x}, \mathbf{x}_0) = \int_{\mathbf{x}_0}^{\mathbf{x}} c\,ds. \tag{11}$$

The integral in (11) is taken along the ray Ω. The function $|Q_2''(\mathbf{x}, \mathbf{x}_0)|$ is the relative geometrical spreading in a plane of the ray Ω and can be evaluated by a 2-D dynamic ray tracing, consisting of 2 equations only.

For a ray Ω crossing N interfaces at points Q_i , i = 1,2,....,N, the ray propagator matrix should be multiplied by a 4×4 interface matrix $\mathbf{F}(Q_i)$ at any point Q_i , to satisfy the boundary conditions. The final expressions for the ray propagator matrix is then as follows,

$$\mathbf{\Pi}(\mathbf{x}, \mathbf{x}_0) = \mathbf{\Pi}(Q_{N+1}, Q_N) \prod_{i=N}^{1} [\mathbf{F}(Q_i)\, \mathbf{\Pi}(Q_i, Q_{i-1})], \tag{12}$$

where the point Q_0 corresponds to $\mathbf{x}_0$ and the point Q_{N+1} to $\mathbf{x}$. For more details on dynamic ray tracing and derivation of all above presented equations see Červený (1987, 1989a).

Finally, the symbol R in (6) denotes the complete reflection/transmission coefficient. It is given by the relation,

$$R = \prod_{i=1}^{N} R(Q_i), \tag{13}$$

where the product corresponds to points Q_1 , Q_2 , ..., Q_N of reflection/transmission along the ray. The reflection/transmission coefficients can be expressed by the following relations:

$$\begin{aligned} R_{refl.} &= (\varrho_2 c_2 \cos i_1 - \varrho_1 c_1 \cos i_2) \,/\, (\varrho_2 c_2 \cos i_1 + \varrho_1 c_1 \cos i_2) , \\ R_{transm.} &= (\varrho_1 \varrho_2 c_1 c_2 \cos i_1 \cos i_2)^{1/2} \,/\, (\varrho_2 c_2 \cos i_1 + \varrho_1 c_1 \cos i_2). \end{aligned} \tag{14}$$

Here c_1 and ϱ_1 are the velocity and density at the point of incidence Q_i, on the side of the incident wave, c_2 , ϱ_2 have the same meaning, but on the opposite side of the interface, i_1 is the angle of incidence, i_2 is the angle of transmission. Note that both $R_{refl.}$ and $R_{transm.}$ are reciprocal, so that the complete reflection/transmission coefficient R given by (13) is reciprocal. Note also a non-traditional form of the reciprocal transmission coefficient in (14).

In the frequency domain, the acoustic Green function $G(\mathbf{x}, \mathbf{x}_0, \omega)$ is a solution of the acoustic wave equation

$$\nabla\cdot(\sigma\nabla G) + \omega^2 \varkappa\, G = -\,\delta(\mathbf{x} - \mathbf{x}_0). \tag{15}$$

The ray theory Green function $G(\mathbf{x}, \mathbf{x}_0, \omega)$ is again given by the summation (4) over all rays Ω, where the elementary Green functions $G^{\Omega}(\mathbf{x}, \mathbf{x}_0, \omega)$ are given by the equation

$$G^{\Omega}(\mathbf{x}, \mathbf{x}_0, \omega) = A^{\Omega}(\mathbf{x}, \mathbf{x}_0)\, e^{i\omega T^{\Omega}(\mathbf{x}, \mathbf{x}_0)}. \tag{16}$$

It should be emphasized that the acoustic ray theory Green function is spatially reciprocal, both in the time domain, see (5), and in the frequency domain, see (16);

$$G(\mathbf{x},t\,;\,\mathbf{x}_0,t_0) = G(\mathbf{x}_0,t\,;\,\mathbf{x},t_0)\,,$$

$$G(\mathbf{x}, \mathbf{x}_0, \omega) = G(\mathbf{x}_0, \mathbf{x}, \omega).$$

BORN APPROXIMATION

Let us consider a model in which the specific volume $\sigma(\mathbf{x})$ and the compressibility $\varkappa(\mathbf{x})$ are given by the equations

$$\sigma(\mathbf{x}) = \sigma_0(\mathbf{x}) + \sigma'(\mathbf{x})\,,$$

$$\varkappa(\mathbf{x}) = \varkappa_0(\mathbf{x}) + \varkappa'(\mathbf{x}). \tag{17}$$

Here $\sigma_0(\mathbf{x})$ and $\varkappa_0(\mathbf{x})$ correspond to the background model, and $\sigma'(\mathbf{x})$, $\varkappa'(\mathbf{x})$ are small perturbations. When a wave is incident on a region of non-vanishing $\sigma'(\mathbf{x})$, $\varkappa'(\mathbf{x})$, a scattered wavefield is generated.

Let us assume that a point source (2) is situated at a point $\mathbf{x} = \mathbf{x}_s$, and the receiver at $\mathbf{x} = \mathbf{x}_r$. Then the Born integral representation of the single scattered acoustic wave field $B(\mathbf{x}_r, \mathbf{x}_s, \omega)$ in the frequency domain is as follows:

$$B(\mathbf{x}_r, \mathbf{x}_s, \omega) = \iiint \{\omega^2 \varkappa'(\mathbf{x})\, G(\mathbf{x}_r, \mathbf{x}, \omega)\, G(\mathbf{x}, \mathbf{x}_s, \omega) - \sigma'(\mathbf{x})\, \nabla G(\mathbf{x}_r, \mathbf{x}, \omega)\, \nabla G(\mathbf{x}, \mathbf{x}_s, \omega)\}\, d\mathbf{x}. \tag{18}$$

The integration is over the whole space V in which $\sigma'(\mathbf{x})$ and $\varkappa'(\mathbf{x})$ are non-vanishing. The symbol G denotes the Green function in the background medium. In the following, we shall consider an asymptotic high-frequency expression for $B(\mathbf{x}_r, \mathbf{x}_s, \omega)$. In other words, in (18) we can use the ray expressions for the Green functions, see (4) and (16). For simplicity, we shall not write the summation (4) and the superscript Ω in the expressions for the Green function, its amplitude and relevant travel time. We will tacitly understand that the summation should be performed over all rays connecting $\mathbf{x}_s$ with $\mathbf{x}$ and $\mathbf{x}_r$ with $\mathbf{x}$. Our expressions will correspond to one, but arbitrary, selection of rays from $\mathbf{x}_s$ to $\mathbf{x}$ and from $\mathbf{x}_r$ to $\mathbf{x}$. Using (16), we can easily obtain an approximate high-frequency equation,

$$\nabla G(\mathbf{x}_r, \mathbf{x}, \omega) = i\omega A(\mathbf{x}_r, \mathbf{x}) \nabla T(\mathbf{x}_r, \mathbf{x}) e^{i\omega T(\mathbf{x}_r, \mathbf{x})},$$

and similarly for $\nabla G(\mathbf{x}_s, \mathbf{x}, \omega)$. This yields

$$\begin{aligned} B(\mathbf{x}_r, \mathbf{x}_s, \omega) = \omega^2 \iiint & \{\varkappa'(\mathbf{x}) + \sigma'(\mathbf{x}) \\ & \times c_0^{-2}(\mathbf{x}) \cos\theta(\mathbf{x}_r, \mathbf{x}_s, \mathbf{x})\} \\ & \times a(\mathbf{x}_r, \mathbf{x}_s, \mathbf{x}) e^{i\omega T(\mathbf{x}_r, \mathbf{x}_s, \mathbf{x})} \, d\mathbf{x}, \end{aligned} \tag{19}$$

where

$$\begin{aligned} a(\mathbf{x}_r, \mathbf{x}_s, \mathbf{x}) &= A(\mathbf{x}_s, \mathbf{x}) A(\mathbf{x}_r, \mathbf{x}), \\ T(\mathbf{x}_r, \mathbf{x}_s, \mathbf{x}) &= T(\mathbf{x}_s, \mathbf{x}) + T(\mathbf{x}_r, \mathbf{x}), \\ \cos\theta(\mathbf{x}_r, \mathbf{x}_s, \mathbf{x}) &= c_0^2(\mathbf{x}) \nabla T(\mathbf{x}_s, \mathbf{x}) \nabla T(\mathbf{x}_r, \mathbf{x}). \end{aligned} \tag{20}$$

All the quantities a, T and $\cos\theta$ are reciprocal. Let us emphasize that the expressions for the amplitudes A and travel times T in (20) can be calculated by ray tracing in the background medium, even inside the volume V.

Several alternative forms of (19) are possible. It is not difficult to show that the perturbation factor in (19) can be written as follows:

$$\varkappa'(\mathbf{x}) + [\sigma'(\mathbf{x})/c_0^2(\mathbf{x})] \cos\theta = -4 \cos^2(\theta/2) R(\mathbf{x}_r, \mathbf{x}_s, \mathbf{x})/c_0(\mathbf{x}) Z_0(\mathbf{x}), \tag{21}$$

where

$$R(\mathbf{x}_r, \mathbf{x}_s, \mathbf{x}) = \tfrac{1}{2}\,\delta Z + \tfrac{1}{2}\,\delta c \tan^2(\theta/2). \tag{22}$$

Here $Z = \varrho c$ is the acoustic impedance, $\delta Z = (Z - Z_0)/Z_0$, $\delta c = (c - c_0)/c_0$; the subscript "0" corresponds to the background medium. The function R corresponds to a linearized form of the reflection coefficient $R_{refl.}$ from (14). Inserting (21) into (19) yields:

$$B(\mathbf{x}_r, \mathbf{x}_s, \omega) = -4\omega^2 \iiint R \cos^2(\theta/2)[c_0(\mathbf{x})\, Z_0(\mathbf{x})]^{-1} \times a(\mathbf{x}_r, \mathbf{x}_s, \mathbf{x})\, e^{i\omega T(\mathbf{x}_r, \mathbf{x}_s, \mathbf{x})}\, dx. \tag{23}$$

The equations (19) and (23) are final expressions for the 3-D Born integral.

In a 2-D case, Born integrals can be simplified. Let us assume that both the background model and the perturbations do not depend on x_2. In other words, the scatterers are infinitely prolongated along the x_2 axis. We also consider the source $\mathbf{x}_s$ and the receiver $\mathbf{x}_r$ situated in the plane $x_2 = 0$, so that $x_{s2} = x_{r2} = 0$. We do not consider a line source, but a point source at $\mathbf{x}_s$; such a configuration is often called a 2.5 dimensional case. Then the integral over x_2 in (19) and (23) can be calculated for high-frequency ω by the method of stationary phase to give

$$B(\mathbf{x}_r, \mathbf{x}_s, \omega) = (2\pi)^{1/2} \omega^{3/2} e^{i\pi/4} \iint \{\varkappa'(\mathbf{x}) + \sigma'(\mathbf{x})\, c_0^{-2}(\mathbf{x}) \cos\theta\} \times a(\mathbf{x}_r, \mathbf{x}_s, \mathbf{x})\, Y(\mathbf{x}_r, \mathbf{x}_s, \mathbf{x})\, e^{i\omega T(\mathbf{x}_r, \mathbf{x}_s, \mathbf{x})}\, dx_1\, dx_3, \tag{24}$$

or, alternatively,

$$B(\mathbf{x}_r, \mathbf{x}_s, \omega) = -4\,(2\pi)^{1/2} \omega^{3/2} e^{i\pi/4} \iint R \cos^2(\theta/2)[c_0(\mathbf{x})\, Z_0(\mathbf{x})]^{-1} \times a(\mathbf{x}_r, \mathbf{x}_s, \mathbf{x})\, Y(\mathbf{x}_r, \mathbf{x}_s, \mathbf{x})\, e^{i\omega T(\mathbf{x}_r, \mathbf{x}_s, \mathbf{x})}\, dx_1\, dx_3, \tag{25}$$

Here the function $Y(\mathbf{x}_r, \mathbf{x}_s, \mathbf{x})$ is given by the relation

$$Y(\mathbf{x}_r, \mathbf{x}_s, \mathbf{x}) = [\,1/\sigma(\mathbf{x}_s, \mathbf{x}) + 1/\sigma(\mathbf{x}_r, \mathbf{x})\,]^{1/2}, \tag{26}$$

σ is given by (11). The integration is over the volume V' which represents a part of the plane $x_1 x_3$ in which δZ and δc are nonvanishing.

For more details on the Born approximation, including the elastodynamic case, see Beydoun and Mendes (1989), Beylkin and Burridge (1990), Coates and Chapman (1990), Wu (1989a,b). These papers also present extensive literature related to this subject.

HYBRID RAY-BORN MODELLING

The hybrid ray-Born modelling can be used to compute synthetic seismograms for laterally varying layered structures, containing scatterers of the size smaller than a prevailing wavelength. The scatterers can be, of course, combined to form bodies of a complex shape. To compute the wavefield corresponding to the background laterally varying layered structure, the ray method is used, and relevant synthetic seismograms are generated. To evaluate the single scattered wave field, eqs. (19) or (23) can be used for 3-D, and eqs. (24) or (25) for 2-D.

The program package BEAM87, see Červený (1989b), is modified to perform such hybrid ray-Born computations in two-dimensional laterally varying layered structures.

The wave field, generated by a point source situated at any point of the model, is computed by the ray method as a superposition of individual elementary waves. The elementary waves may be selected by the user (direct, reflected, transmitted, multiply reflected/transmitted). Zero-order approximation of the ray method is used in the computation.

The scatterers may be also situated at arbitrary positions. The elementary wave incident on the scatterer and generating the single scattered field may be again selected arbitrarily, similarly as the rays along which the scattered waves propagate from the scatterer to the receiver. The single scattered wave field is calculated by Born integrals.

NUMERICAL EXAMPLES

In the numerical examples, we shall consider a simple laterally varying 2-D background model with two curved interfaces (see Fig. 1). The velocity c in all layers is increasing downwards, and also laterally from the left to the right. The average velocities in the first layer are close to 3 km/s, in the second layer close to 4 km/s, and in the last layer close to 5 km/s. For example, in the first layer, the velocity changes from 2.7 km/s in the top left-hand corner of the

layer to 3.6 km/s in the bottom right-hand corner of the layer. The density is constant in the whole model, and the absorption is not considered.

In the model, the x_1-axis of the Cartesian coordinate system is taken along the upper boundary of the model, which is pressumably planar, and is situated inside the medium. (The effects of the surface are not taken into account). The x_3-axis of the Cartesian coordinate system is oriented downwards, the coordinate x_3 corresponds to depth. The receivers are distributed along the upper boundary of the model. The point source is situated at $x_1 = 2$ km, $x_3 = 0$ km. The source time function corresponds to the Gabor signal

$$x(t) = \exp [- (2 \pi f_M t/\gamma)^2] \cos (2 \pi f_M t + \upsilon),$$

with $\gamma = 4$, $f_M = 30$ Hz, $\upsilon = 0$. The scatterers are situated in different parts of the model in individual presented examples.

The ray-Born method has been used to evaluate the wave field at individual receivers. The standard ray method has been applied in the calculation of the waves reflected from both interfaces in the background model, and the scattered wave field from the scatterers was evaluated by the Born approximation.

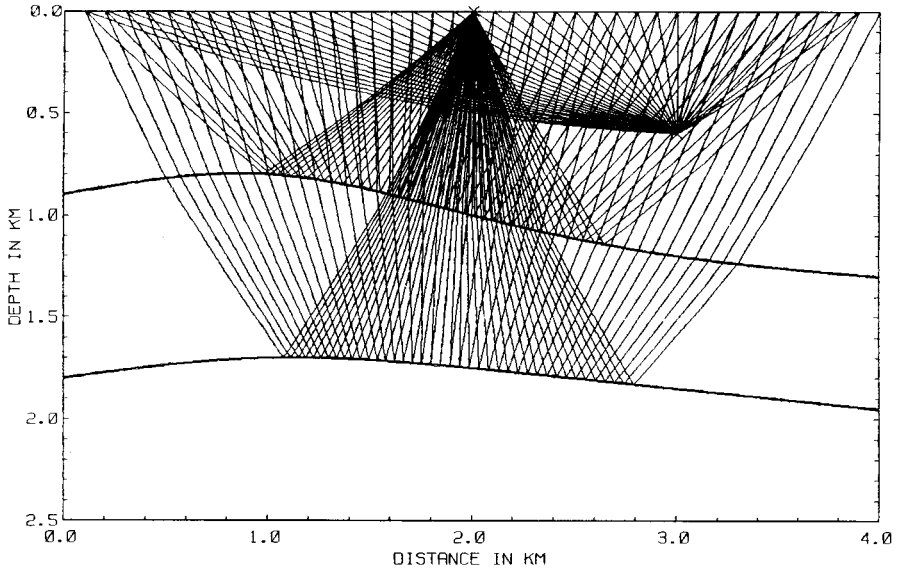

Fig. 1. A 2-D laterally varying structure with two curved interfaces and one single scatterer. A point source is situated in the middle of the upper boundary of the model. Ray diagrams of waves reflected from both interfaces and of the scattered wave are shown.

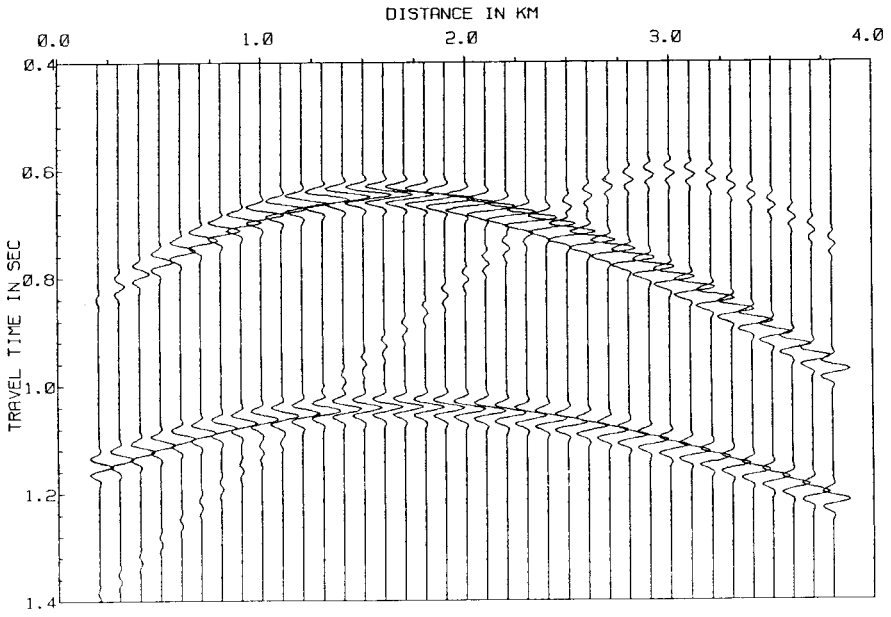

Fig. 2a. Ray-Born synthetic seismograms for the model corresponding to Fig. 1. The size of the scatterer is 25 × 25 m, and the velocity within the scatterer is by 10% higher than in the background model.

In the **first example**, the scatterers are situated close to the point $x_1 = 3$km, $x_3 = 0.6$ km. Fig. 1 shows the ray diagrams of waves reflected from both interfaces, and a ray diagram corresponding to one scatterer of the size $\Delta x_1 = \Delta x_3 = 25$ m, situated at $x_1 = 3.0$ km, $x_3 = 0.6$ km. The scatterer is, of course, infinitely prolongated along the x_2 axis. The velocity c within the scatterer (in the perturbed model) differs by 10% from the velocity in the background medium. The ray-Born synthetic seismograms for the model with the above described scatterer are shown in Fig. 2a. All the synthetic seismograms are normalized with respect to the maximum amplitude in the whole section. The scattered wave field has a simple hyperbolic appearence. A very interesting behaviour of the scattered wave field is a slow decrease of amplitudes along very long tails of the diffraction hyperbola. Fig. 2b shows the ray-Born synthetic seismograms corresponding to a thin plate scatterer situated roughly at the same place as the individual scatterer considered in Figs. 1 and 2a. The thickness of the plate is 25 m, and its length 275 m. Note that the wavelength in this part of the model is close to 110 m. The scatterer is again infinitely prolongated along the x_2 axis. The plate makes approximately an angle

of 45° with the x_1 and x_3 axes. From a numerical point of view, the plate scatterer is approximated by eleven individual scatterers. The velocity inside the scatterer is the same as in the individual scatterer in Fig. 2a. It is interesting to observe that the scattered wave field corresponding to a thin plate is of a different character than the scattered wave field corresponding to a single scatterer. The tails corresponding to individual scatterers forming the plate scatterer are mutually cancelled by a destructive interference. Only two tails are formed, corresponding to its end points. The tail amplitudes are weaker in this case than in Fig. 2a. In between, a regular reflected wavefield from the scattering thin plate is formed, see receivers at x_1 = 2.5 - 3 km. The scattered wave field is very intensive, comparable with the intensity of waves reflected from the two interfaces.

Several similar numerical experiments have been performed with different shapes and orientations of combined scatterers. In general, the amplitudes of the scattered wave field recorded on the surface of the model depend considerably on the orientation of the (plate) scatterer. The scattered wave field is rather strong for horizontal scatterers, but considerably weaker for vertical scatterers.

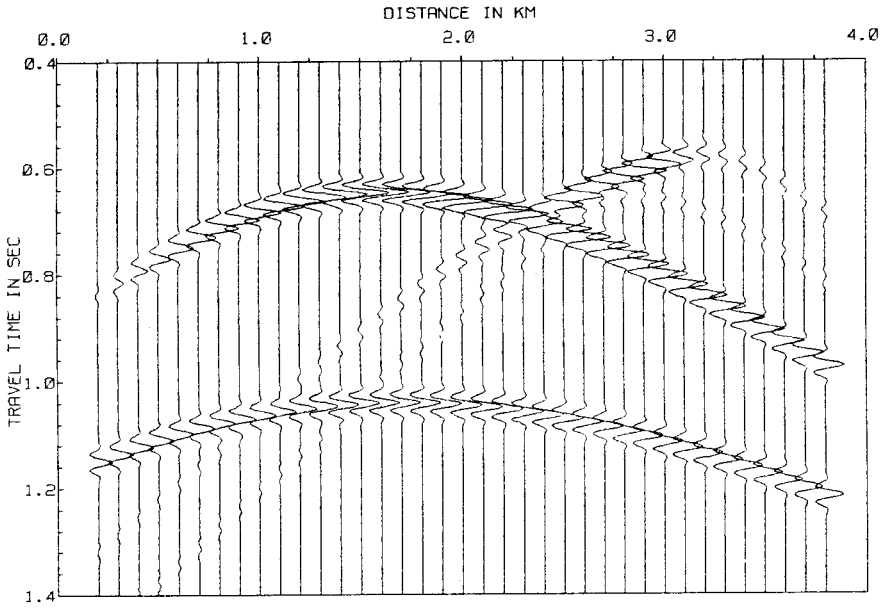

Fig. 2b. Ray-Born synthetic seismograms for the same configuration as in Fig. 2a, only the single scatterer is replaced by a scattering plate of the size 275 × 25 m, composed of 11 individual scatterers. The plate makes an angle of 45° with the x_1 and x_3 axis.

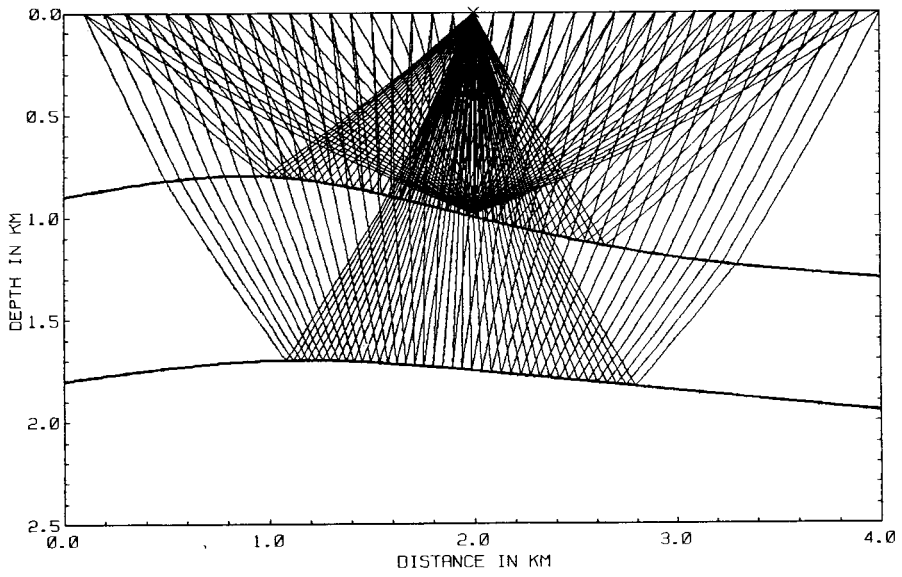

Fig. 3. Ray diagrams for the same structure as in Fig. 1, only the scatterer is situated directly above the first interface, in the first layer.

In the **second example**, the scatterers are situated directly on the upper side of the first interface. For one scatterer of the size $\Delta x_1 = \Delta x_3 = 25$ m, the ray diagram is shown in Fig. 3. In Figs. 4a,b,c, the ray-Born synthetic seismograms are shown, corresponding to different scatterer configurations. The velocity within scatterers corresponds to the velocity below the interface. The synthetic seismograms are again normalized with respect to the maximum amplitude in the whole section. Fig. 4a corresponds to one scatterer, see the ray diagrams on Fig. 3. Fig. 4b simulates a corrugated interface of a length of 325 m, between $x_1 = 1.8$ km and $x_2 = 2.1$ km. The scatterers, of a size of 25m, are situated along the interface, also with gaps of 25 m. Finally, Fig. 4c shows a continuous system of scatterers of a length of 325 m, without gaps. Thus the last model represents an elevation of the interface by 25 m in the total length of 325 m, with sharp edges at both sides of the elevation.

The wave field corresponding to a single scatterer in Fig. 4a is simple. The decrease of amplitudes along long tails is again very slow. The wavefields corresponding to the corrugated interface (Fig. 4b) and to the elevated interface

(Fig. 4c) are, of course, mutually very different. The corrugated interface generates strong and long reverberations, see the L.H.S. of Fig. 4b. It also destroys the regular reflected wave field at certain receivers, see e.g., receivers at x_1 = 3.2 - 3.4 km in Fig. 4b. On the other side, the local elevation of the interface does not yield such a strong scattered field (see Fig. 4c). The reverberations are considerably supressed. The local elevation generates only two scattered waves from the edges of the elevation. If we compare the arrival times of reflected waves at $x_1 \sim$ 2.0 - 2.5 km in Figs. 4a and 4c, we can clearly observe the earlier arrivals in Fig. 4c, due to the elevated interface. Close to both edges of the elevation, the reflected wave field is considerably influenced by the edge effects. See the traces at x_1 = 1.6 - 1.9 km and at x_1 = 3.0 - 3.4 km. For other examples of computations, see Coppoli D.M. (1991).

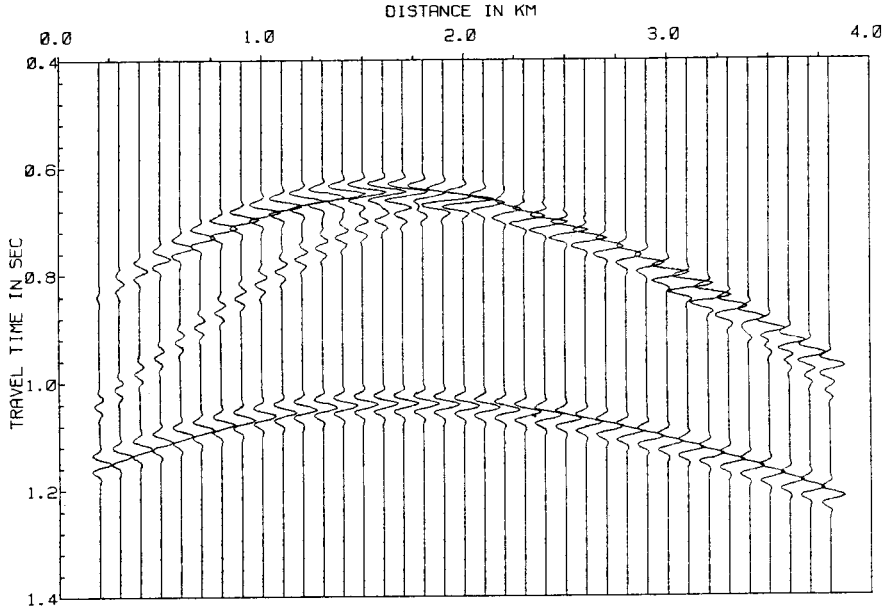

Fig. 4a. Ray-Born synthetic seismograms for the model corresponding to Fig.3. The size of the scatterer is 25 × 25 m. The velocity within the scatterer correspond to the velocity below the interface, in the second layer.

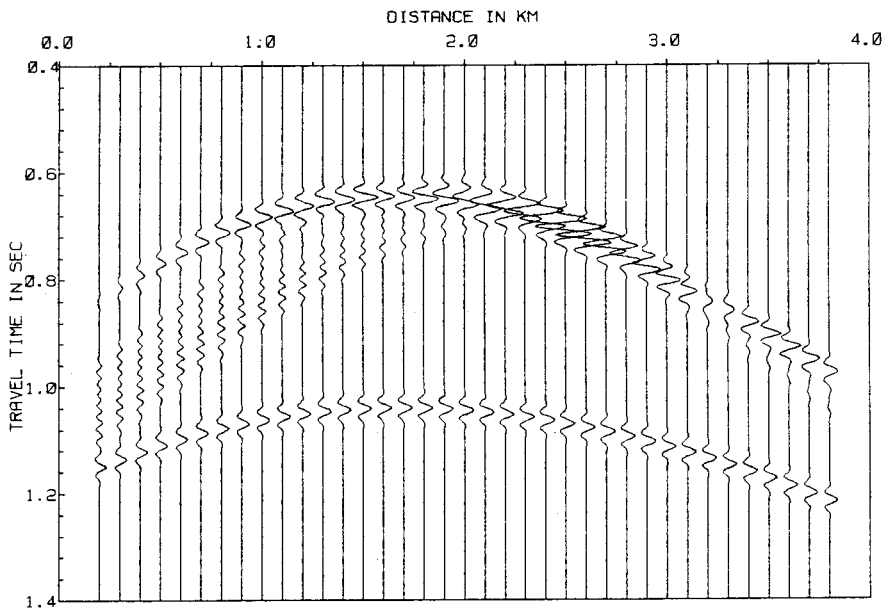

Fig. 4b. Ray-Born synthetic seismograms for the same configuration as in Fig. 4a, only a single scatterer is replaced by a system of seven scatterers. These individual scatterers form a corrugated interface of the length of 325 m. The scatterers are of the size of 25 × 25 m, the distance between them is also 25 m.

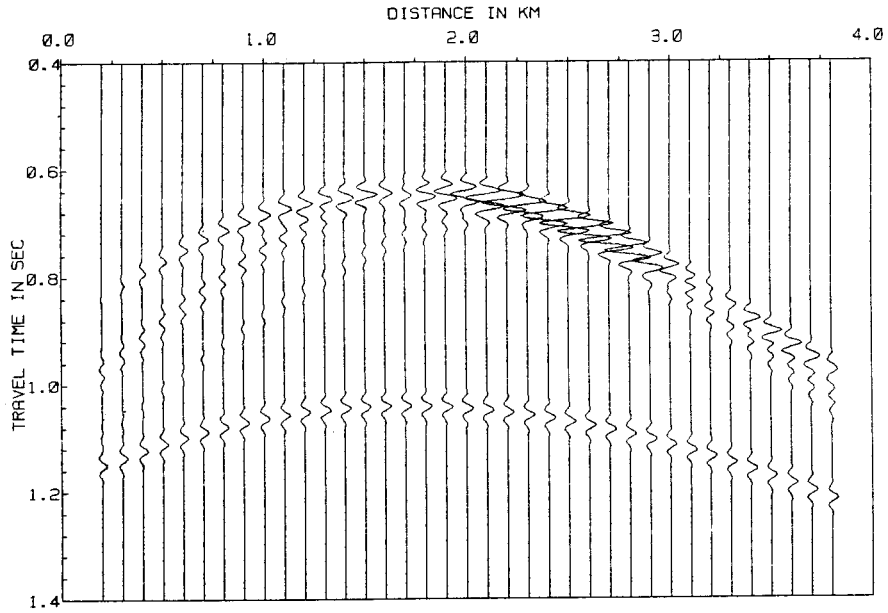

Fig. 4c. Ray-Born synthetic seismograms for the same configuration as in Fig. 4b, but the system of scatterers is continuous along the interface and simulates a continuous elevation of the interface in the length of 325 m. The elevation is formed by 13 single scatterers.

CONCLUSIONS

As we have shown, the numerical modelling of high-frequency seismic wave fields in 2-D laterally varying layered structures containing small scatterers can be simply performed by the combination of the ray theory with the Born approximation. Even though the presented numerical examples are very simple, the method could be applied to considerably more complex situations, e.g. to a random distribution of horizontal and/or vertical scatterers within some region, to combined scatterers of an arbitrary shape, etc. To simplify the explanations, only the acoustic case is discussed here, but the modification for an elastic isotropic and/or elastic anisotropic case is straightforward. Similarly, any algorithm for 3-D ray computations could be simply generalized to include the 3-D ray-Born modelling. The proposed method has several important limitations. It can only be used if the perturbations of the model are weak and if the wave field is of a high-frequency character. Moreover, only the single scattering is considered; multiple reflections between individual scatterers and inside the bodies of complex shape are not obtained.

ACKNOWLEDGEMENTS

This work was done during the first author's stay at the Federal University of Bahia, Salvador. The research was sponsored by the CNPq, FINEP, PETROBRAS and by the IBM Academic Initiative in Czechoslovakia.

REFERENCES

Beydoun, W.B. and M. Mendes, 1989. Elastic ray-Born l_2-migration/inversion. J. Geophys. Res., 97: 151-160.

Beylkin, G. and Burridge, R., 1990. Linearized inverse problems in acoustics and elasticity. Wave Motion, 12: 15-52.

Červený, V., 1987. Ray methods for three-dimensional seismic modelling. Lecture notes, The University of Trondheim and The Norwegian Inst. of Technology, Trondheim, Norway.

Červený, V., 1989a. Seismic ray theory. In: Encyclopedia of Solid Earth Geophysics, D.E. James (ed.), pp. 1098-1118, Van Nostrand Reinhold Co., New York.

Červený, V., 1989b. Synthetic body wave seismograms for laterally varying media containing thin transition layers. Geophys. J. Int., 99: 331-349.

Coates, R.T. and C.H. Chapman, 1990. Ray perturbation theory and the Born approximation. Geophys. J. Int., 100: 379-392.

Coppoli D.M., A., 1991. Ray-Born synthetic seismograms for complex structures containing scatterers. M.Sc. Thesis, PPPG/Federal University of Bahia, Salvador.

Wu, Ru-Shan, 1989a, Seismic wave scattering. In: Encyclopedia of Solid Earth Geophysics, D.E. James (ed.), pp. 1166-1187, Van Nostrand Reinhold Co., New York.

Wu, Ru-Shan, 1989b. The perturbation method in elastic wave scattering. Pageoph, 131: 605-637.